18

Investigating the Performance of Intensive Mammalian Cell Bioreactor Systems Using Magnetic Resonance Imaging and Spectroscopy

KEVIN M. BRINDLE

Department of Biochemistry, University of Cambridge, 80 Tennis Court Road, Cambridge CB2 1GA, UK

Introduction

Intensive bioreactor systems, i.e. systems which maintain cells at relatively high densities, have been widely used as production systems for monoclonal antibodies and recombinant proteins. These systems include packed and fluidized beds, in which the cells are grown attached to the bed matrix, and spin filters, in which the cells are retained within a filter in a conventional stirred tank system (Himmelfarb *et al.*, 1969; Glacken *et al.*, 1983; Arathoon and Birch, 1986). An important and popular intensive reactor system has been the hollow fibre bioreactor (HFBR) (Knight, 1989). Medium pumped through the fibres exchanges nutrients and waste products with cells growing in the extracapillary space. The principal advantages of the HFBR as a production system, over for example more conventional stirred tank reactors, include maintenance of higher cell densities, concentration and isolation of cell products prior to harvest and an increased per-cell productivity. These systems are also finding use in the burgeoning field of tissue engineering (Langer and Vacanti, 1993; Hubbell and Langer, 1995; Langer and Vacanti, 1995). In this case they can be used to grow up large quantities of cells for transplant, or the cell-loaded devices can themselves be used as implanted or extra-corporeal bioartificial organs. A well-known example are hepatocyte-loaded reactors which can be used as artificial livers (Yarmush *et al.*, 1992; Jauregui *et al.*, 1996; Kamlot *et al.*, 1996). In this case, the important advantage of the intensive reactor is its capability to maintain a high concentration of cells, which can be perfused with the patients blood. In the context of conventional tissue culture, the number of cells required is enormous. It has been suggested that liver function can be maintained with as little as 10% of total liver mass (Kamlot *et al.*, 1996); however, in a 70 kg man this 10% corresponds to ~1.5×10^{10} hepatocytes.

The principal problem of intensive reactor systems is the possibility that gradients

Biotechnology and Genetic Engineering Reviews – Vol. 15, April 1998
0264–8725/98/15/499–520 $20.00 + $0.00

of nutrients and waste products may be formed. For example, in hollow-fibre bioreactor systems gradients can form both radially, where nutrient concentration declines with distance from the fibre wall and also axially, where the concentration declines along the length of the fibre (Chresand *et al.*, 1988; Drury *et al.*, 1988; Piret and Cooney, 1990a; Piret and Cooney, 1990b). This problem is particularly acute in the case of oxygen, which has a relatively low solubility in tissue culture medium. Lack of oxygen or anoxia can have a significant impact on reactor function. For example oxygen tension has been shown to limit hepatocyte attachment and subsequent spreading on a collagen substrate (Rotem *et al.*, 1994). As well as affecting cell growth, anoxia may also significantly perturb cell metabolism. This is likely to be an important problem in the case of artificial organs, such as the artificial liver, where cellular metabolism is intimately involved in the cells' function as a surrogate organ. Poor oxygen delivery is less likely to be a problem in reactors used as production systems, for recombinant proteins and antibodies, etc., as the cells used in these systems, such as hybridomas, myelomas and CHO cells, have much lower oxygen consumption rates than hepatocytes (Peng and Palsson, 1996). For example, the oxygen uptake rate of hepatocytes is around 1.0 μmol/10^6 cells/h (Rotem *et al.*, 1992), whereas the rate measured in a hybridoma cell line was 0.13 μmol/10^6 cells/hr(Sardonini and DiBiasio, 1992). The relationship between function in these systems i.e. the production of a protein, and the metabolism of the cells may also be more remote. For example, in the case of a hybridoma cell line, the specific antibody production rate was not significantly affected by oxygen limitation during rapid cell growth, although the viable cell concentration was markedly reduced (Shi *et al.*, 1993).

Productivity, however, is not the only important issue here. Another is the quality of the protein product in terms of its homogeneity. The pH of the growth medium and the glucose concentration have been shown to affect the glycosylation patterns of recombinant proteins secreted by CHO cells (Borys *et al.*, 1993; Hayter *et al.*, 1993). Oxygen tension could also affect glycosylation through possible effects on glucose consumption and reactor pH (Shi *et al.*, 1993). Clearly, if there are gradients of these factors in an intensive reactor, then these could increase the heterogeneity of protein glycosylation and thus degrade the quality of the product.

In order to improve the performance of intensive bioreactors, both as artificial organs and as production systems, it is necessary to be able to monitor the effect of reactor design and operation on the formation of nutrient and waste product gradients, and the effects that these have on the metabolism of the cells. Non-invasive NMR spectroscopy and imaging techniques have the capability to measure nutrient and waste product concentrations and the metabolism of the cells in specific regions of functioning and intact intensive bioreactor systems. The purpose of this brief review is to describe the basic principles of NMR spectroscopy and imaging, the type of information that is obtainable using these techniques, how they have been applied to intensive reactor systems and also how they may be applied in the future. The application of NMR techniques to the study of bioreactor systems has been the subject of a number of reviews (Gillies *et al.*, 1989; Donoghue *et al.*, 1992; Fernandez, 1996).

The NMR experiment

A full description of the methodology is beyond the scope of this review and only the

basic principles will be discussed here. More detailed descriptions can be found in the following texts (Derome, 1987; Sanders and Hunter, 1987; Gadian, 1995).

Some nuclei have the property of spin and consequently possess a magnetic moment. In the presence of an applied magnetic field these nuclei assume a number of discrete energy levels determined by their spin quantum number. For spin 1/2 nuclei, which includes many of the commonly studied nuclei such as ^{1}H, ^{31}P, ^{13}C and ^{15}N, there are two allowed energy levels, in which the nuclear magnetic moments are aligned with (the lower energy level) or against (higher energy level) the applied field. The magnetic moments do not align exactly with the applied magnetic field but precess around it with a frequency which is dependent on the nucleus and the strength of the applied field (see *Figure 1*).

$$\nu = \frac{|\gamma| B_0}{2\pi} \tag{1}$$

where ν is the precessional or Larmor frequency in hertz, γ is the gyromagnetic ratio of the nucleus and B_0 is the strength of the applied magnetic field.

If an oscillating magnetic field is applied perpendicular to the main field, B_0, at a frequency which is equal to the precessional frequency of the nuclei, i.e. is resonant with this frequency, then transitions are induced between the two energy levels. This is the phenomenon of nuclear magnetic resonance. When thinking about the NMR experiment it is often convenient to consider what happens to the bulk magnetization in the sample. As there is a slight excess of spins in the lower energy level, whose magnetic moments are aligned with the field, there is a net magnetization vector which lies along the B_0 field direction or z axis (see *Figure 1*). The oscillating magnetic field, which induces transitions between the two energy levels, tips this vector (M_z) away

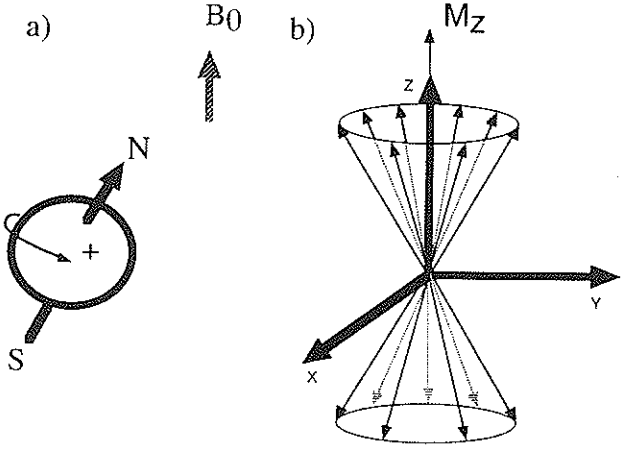

Figure 1. a) A rotating charged nucleus creates a magnetic field and is equivalent to a small bar magnet whose axis is coincident with the spin rotation axis. When placed in a strong magnetic field (B_0), the nuclei do not align exactly in the direction of the applied field but precess about it. b) The many precessing spins in the sample can be considered to have a common origin. At equilibrium there is an excess of spins oriented along the B_0 field direction (the lower energy level, see text), thus producing a net magnetization vector, M_z, which lies along the +z axis.

Table 1. Properties of nuclei commonly detected in NMR experiments *in vivo*

Nucleus	Spin quantum number	Frequency at 9.4 T (MHz)	Natural abundance %	Relative sensitivity for equal number of nuclei at constant field (% vs. ^{1}H)
^{1}H	1/2	400.0	99.98	100
^{13}C	1/2	100.6	1.108	1.59
^{15}N	1/2	40.5	0.365	0.104
^{19}F	1/2	376.3	100.0	83.3
^{23}Na	3/2	105.8	100.0	9.25
^{31}P	1/2	161.9	100.0	6.63

Data taken from (James, 1975).

from the z axis into the x,y, plane, where it can be detected by the NMR receiver coil. This is usually the same coil that is used to apply the exciting or B_1 magnetic field. When the B_1 field is turned off, the magnetization in the x,y plane decays, with a time constant T_2, known as the spin–spin relaxation time, and returns to the z axis with a time constant T_1, known as the spin lattice relaxation time. The bulk magnetization, M_z, can be rotated to varying degrees about the applied B_1 field, depending on its strength and duration. Maximum signal will be obtained when M_z is flipped through 90^0 so that it lies fully within the x,y plane. Under these circumstances the applied B_1 field is referred to as a 90^0 pulse. The duration of the excitation pulse is typically several μsec. The decaying magnetization, which follows the pulse, induces a signal in the receiver coil, which is digitized by the acquisition computer.

Different nuclei precess at different frequencies. The precessional frequencies of some commonly detected nuclei, at a field of 9.4 T, is given in *Table 1*. (Also given are their relative sensitivities to NMR detection.) This magnetic field is one which is in common use in high field NMR studies of intact biological systems, such as small mammals, perfused organs and isolated cells. The limit on the size of sample, at this relatively high field, is imposed by the available bore size of the magnet. The bore of a 'wide-bore' 9.4 T magnet is typically 89 mm. The available bore, however, when the magnetic field shims and gradients (for imaging) have been inserted, is much less, typically of the order of 40 mm. Furthermore, the magnetically homogenous volume within this space is even smaller. When making measurements on cells, on our 9.4 T instrument, we use a sample diameter of 25 mm and measure signal from a length of approximately 30 mm. Magnets used for clinical spectroscopy have much larger bores (but lower field strengths).

CHEMICAL SHIFT

Fortunately for the chemist and biochemist, each nucleus does not precess at a single frequency but over a range of frequencies determined by its chemical or electronic environment. For the phosphorus nucleus, in biologically relevant molecules, this spread of frequencies is typically of the order of several kHz at a field of 9.4 T. When the B_1 field is applied in the form of a short, high intensity pulse, it does not excite a single frequency but a range of frequencies, the bandwidth of which is inversely proportional to the duration of the pulse and is typically several kHz. Thus the excitation pulse can excite the entire spectrum of resonance frequencies of a particular nucleus present in the sample. The different frequency components of the signal

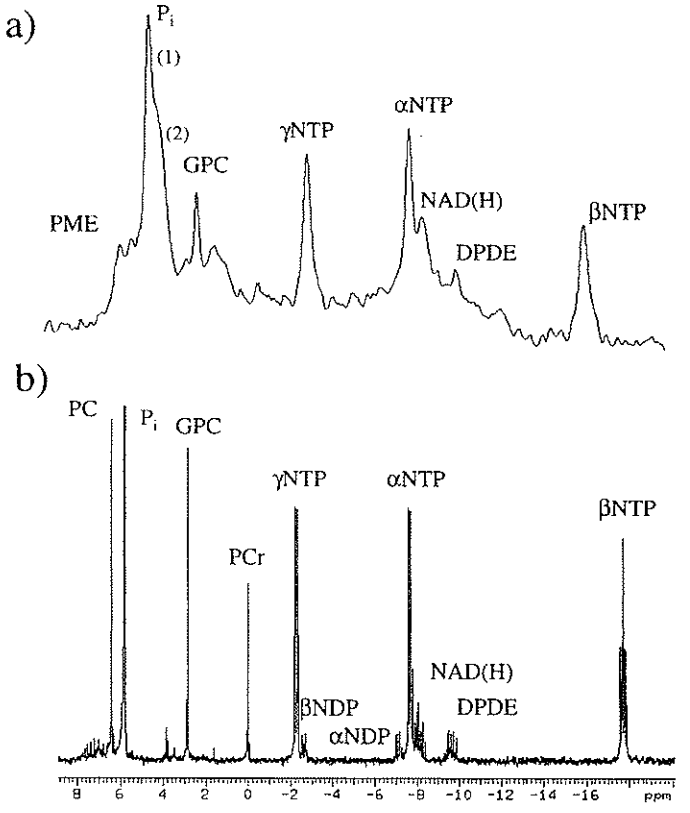

Figure 2. (a) ^{31}P NMR spectrum of CHO-K1 cells growing in a hollow-fibre bioreactor. The cell density in the reactor was approximately 1×10^8 cells/ml and the spectrum took 47 minutes to acquire. Note that the P_i peak has two components (labelled 1 and 2), indicating that there are two components in the reactor of differing pHs. (b) High resolution ^{31}P NMR spectrum of a perchloric acid extract prepared from approximately 1×10^9 CHO-K1 cells. The spectrum is the sum of 10 000 transients and took 14 hours to acquire. Abbreviations: PME, phosphomonoesters; PDE, phosphodiesters; γ-, α- and β-NTP, γ-, α- and β-phosphates, respectively, of nucleoside triphosphates; β- and α-NDP, β- and α-phosphates respectively of nucleoside diphosphates; DPDE, diphosphodiesters. The nucleoside phosphates are predominantly ATP and ADP.

obtained after the pulse can be deconvoluted by Fourier transformation and displayed as a spectrum. The ^{31}P spectrum shown in *Figure 2a* was obtained from Chinese Hamster ovary (CHO) cells growing in a hollow fibre bioreactor. The frequency of each resonance, which is displayed on the x axis, is characteristic for the nucleus in a particular chemical environment. Thus the ^{31}P nuclei in the three phosphates of ATP resonate at significantly different frequencies. The frequency or chemical shift (δ) of these resonances is expressed as parts per million (ppm) of the operating frequency of the spectrometer. For ^{31}P at a field of 9.4 T this is 161 MHz.

$$\delta = \frac{(\nu_{ref} - \nu_{sample}) \times 10^6}{\nu_{instr.}} \qquad (2)$$

where $\nu_{instr.}$ is the operating frequency of the spectrometer and $\nu_{ref} - \nu_{sample}$ is the difference in the resonance frequencies of a reference (see below) and the sample

resonances. The advantage of expressing chemical shifts in this way is that they are independent of the magnetic field strength B_0, and thus spectra acquired at different field strengths can be compared directly. The amplitudes of the peaks in the spectrum are directly proportional to the number of nuclei giving rise to them.

SENSITIVITY

For many NMR experiments, the signal acquired from a single pulse-acquire cycle is insufficient and further cycles may be required to give adequate signal-to-noise in the resulting spectrum or image. Although the signals add linearly with the number of cycles, the noise adds as the square root and therefore signal-to-noise only improves as the square root of the number of signal acquisitions, i.e. to double the signal-to-noise the number of transients acquired must be increased by a factor of 4. Lack of sensitivity is arguably the most important problem in applying NMR techniques to intact biological systems. Lack of sensitivity places a limit on the concentrations of metabolites which can be detected and also limits the spatial resolution in localized spectroscopy and imaging experiments (see below). A frequently asked question is just how sensitive is the technique? There is no simple answer as it depends on many factors including sample size, cell density, nucleus to be detected (see *Table 1*), field strength and also the temporal resolution required. However, some idea of sensitivity, at least for ^{31}P NMR, can be gained from *Figure 2a*. This spectrum was obtained from approximately 10^9 cells in a volume of 9 ml and is the sum of 2000 transients, which took 47 minutes to acquire. The intracellular ATP concentration was about 3 mM. Sensitivity can be improved by increasing the size of the sample and/or by using a higher field strength. The limit on size is imposed by the volume over which the magnetic field is homogeneous (see above). Currently, the highest field 'wide-bore' instrument, which is commercially available, operates at 11.7 T, which corresponds to a proton frequency of 500 MHz.

SIGNAL QUANTITATION

Peak intensity in a spectrum is proportional to the number of nuclei giving rise to the peak. However, this proportionality may vary between different peaks or resonances depending on the conditions of signal acquisition. If an excitation pulse is applied before the magnetization has had time to recover to its equilibrium position along the z axis, following the preceding excitation pulse, then the amount of signal acquired will be reduced. This is known as signal saturation. If the pulse repetition rate is relatively high and the different resonances in the spectrum have different spin–lattice relaxation times (T_1), then their relative intensities in the spectrum will not be equal to their relative concentrations. This problem can be circumvented by acquiring the signals more slowly and thus allowing the magnetization to relax to equilibrium between pulses. However, this requires a pulse repetition rate which is 4–5× the longest T_1 in the sample. Since the T_1s of phosphorus nuclei *in vivo* can be of the order of 1–2 seconds, this slows significantly the rate of data acquisition. Alternatively, the T_1s can be measured and the signal intensities corrected for signal saturation. Under both these circumstances, the peak intensities can be converted into concentrations. In the case of the ^{31}P spectrum of CHO cells shown in *Figure 2a*, the concentrations of

the phosphorus metabolites were estimated by comparing their peak areas with that of an external standard, methylene diphosphonate, whose resonance is well separated from the other resonances in the spectrum (not shown in the Figure).

RESOLUTION

Figure 2a also illustrates another problem with NMR measurements *in vivo* and that is the lack of spectral resolution. Some of the peaks in this spectrum overlap, for example the phosphomonoester (PME) peak contains contributions from phosphoethanolamine, phosphocholine and sugar phosphates. Spectral resolution can be improved by increasing the strength of the B_0 field, which increases the frequency separation between the resonances. Poor spectral resolution is a particular problem at the relatively low magnetic field strengths commonly used for studies on humans (1.5–2 T). However, field strength is not the only problem. The line widths *in vivo* can be quite large and can significantly degrade spectral resolution. This is illustrated by comparing the ^{31}P NMR spectrum of CHO cells in *Figure 2a* with the ^{31}P NMR spectrum of an acid extract of the same cells shown in *Figure 2b*. Several factors can contribute to the large line widths *in vivo*. These include binding of the observed metabolites to paramagnetic ions and macromolecules. This significantly shortens the T_2 relaxation times of the resonances from these small molecules, and results in broadening of these resonances in the Fourier-transformed spectrum. Note that signals from very large phosphorylated molecules and assemblies, such as nucleic acids and membranes, are not observed in these spectra, as their resonances are broadened beyond detection. However they may be observed at low magnetic field strengths (Murphy *et al.*, 1989). Line widths are also increased *in vivo* by the magnetic inhomogeneity of the sample.

All these factors, which increase line width, can be removed by making an extract of the tissue. As well as increasing resolution, this has the added advantage that the temporal restrictions on data acquisition are relaxed and therefore acquisitions can be longer and the signal-to-noise improved. Measurements on extracts are invaluable for assigning the resonances observed *in vivo*. Resonance assignment typically involves acquiring spectra prior to, and following, the addition of the suspected compound to the extract. If the resonance to be assigned is poorly resolved from other resonances in the spectrum, then assignment might also involve pH titrations, before and after compound addition, and treatment of the extract with an enzyme known to degrade or specifically modify the suspected compound.

The obvious disadvantages of making measurements on tissue extracts are that the tissue may not be readily sampled, e.g. cells in a hollow-fibre bioreactor, the opportunity for sequential measurements on the same system is lost and important information may be lost during the extraction procedure. In the case of ^{31}P NMR, the levels of P_i in the extract frequently exceed those measured *in vivo* due to hydrolysis of organic phosphates during the extraction procedure. There may also be compartmentation of the metabolite, which reduces the visibility of its resonance(s) in the spectrum acquired *in vivo*, but which are fully visible in a spectrum of an extract. For example, the resonances from ADP are readily observed in ^{31}P NMR spectra of tissue extracts but are rarely observed *in vivo*. In muscle the lack of visibility is thought to be due to its binding to actin, while in liver compartmentation within mitochondria

may be responsible (Balaban, 1984; Murphy *et al.*, 1988; Masson and Quistdorff, 1992). Nevertheless, the improved sensitivity and spectral resolution which can be obtained with extracts make this a valuable approach for investigating metabolism, especially when carried out in conjunction with experiments *in vivo*.

SPIN–SPIN COUPLING

Nuclei with a magnetic moment may interact with other nuclear spins resulting in mutual splitting of their signals into multiplets. Close inspection of the ATP resonances in *Figure 2b* shows that the ATP resonances are split. The number of components into which a signal is split is $2nI + 1$, where I is the spin quantum number of the nucleus and n is the number of other nuclei interacting with the nucleus. So, for phosphorus, which is spin 1/2, the β-phosphate resonance of ATP is split into a triplet due to coupling with both the γ- and α-phosphate resonances, while the γ- and α-phosphate resonances are doublets due to their coupling with the β-phosphate resonance. The α-phosphate resonance is also spin–spin coupled to protons on the ribose ring; however, the effects of this coupling have been removed in this spectrum by a procedure known as spin-decoupling. The details of this need not concern us here, suffice it to say that it can be used to improve spectral resolution. An important feature of spin–spin coupling is that the peak splitting is independent of the magnetic field strength.

Although spin–spin coupling is rarely observed *in vivo*, because of poor spectral resolution, its observation *in vitro* is frequently used as an aid to resonance assignment. Spin–spin coupling can also be exploited to enhance the detection of less sensitive nuclei. For example, the incorporation of ^{13}C labels into cellular metabolites can be observed in the ^{1}H spectrum of these metabolites as splitting of the coupled ^{1}H resonances (Brindle *et al.*, 1982; Rothman *et al.*, 1992). As the ^{1}H is more sensitive to NMR detection than ^{13}C (see *Table 1*), the sensitivity of ^{13}C label detection is increased over that which would be obtained with direct detection using ^{13}C NMR. In the case of ^{1}H-^{13}C spin coupling the splitting of the ^{1}H resonances is often large enough that it can be observed in ^{1}H spectra acquired *in vivo*. In addition to enhancing the sensitivity of detection of the less sensitive nucleus, indirect detection via the ^{1}H spectrum also gives the fractional labelling, or in radio-chemical terms the specific activity, of the labelled metabolite. This can be very useful when analysing label fluxes in metabolic pathways. The lack of sensitivity of NMR detection means that, unlike with radioisotopes, the fractional labelling with stable isotopes, such as ^{13}C and ^{15}N, must be relatively high before the isotopes can be detected. Furthermore, the metabolite into which they are incorporated must be present at relatively high concentrations.

Label detection is straightforward when splitting in the ^{1}H spectrum is large but can be a problem when the splitting is much smaller, as is the case with ^{1}H-^{15}N spin coupling. There are, however, NMR experiments or pulse sequences which convert the splitting of the ^{1}H resonance into modulation of its phase. The resultant changes in amplitude of the ^{1}H signal are readily detected. These experiments can also be used to improve spectral resolution by spreading the ^{1}H signals over two or more frequency dimensions (see, for example, Street *et al.* (1993)).

NMR IMAGING AND LOCALIZED SPECTROSCOPY

Equation 1 shows that the frequency of a resonance is linearly dependent on the

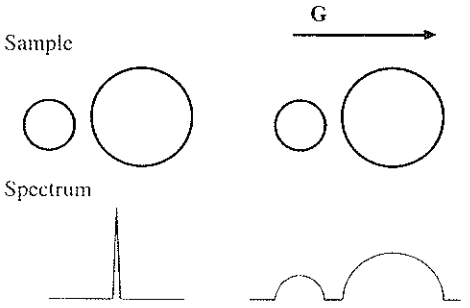

Figure 3. Basic principles of NMR imaging. In a uniform magnetic field there is a single ^1H resonance from the water molecules in the two spheres. If a linear magnetic field gradient (G) is applied to the sample then the resonant frequencies of the protons will be dependent on the position of the water molecules in the field gradient. The spectrum obtained by Fourier transformation is effectively a projection of the sample in the direction of the gradient.

strength of the applied field, B_0. Consider two water-filled spheres (see *Figure 3*). If the B_0 field is uniform across the sample, then the ^1H spectrum will contain a single resonance from the water protons. If, however, we apply a magnetic field gradient, such that the B_0 field strength varies as a linear function of spatial position, then the resonance frequency of the water protons will also vary as a linear function of spatial position. In other words space is frequency-encoded. Water protons in one sphere will resonate at a different frequency to those in the other. Furthermore protons within the spheres will resonate at different frequencies depending on their position such that the Fourier-transformed spectrum is, in effect, a projection of the sample in the direction of the gradient (see *Figure 3*). By applying the gradient in several different directions, the resulting projections can be used to construct an image of the sample. Although the first NMR images were acquired in this way, this technique is rarely used today. Nevertheless, it illustrates very well the basic principles of NMR imaging. Discussion of current methods, which is beyond the scope of this chapter, can be found in the following (Pykett, 1982; Kuhn, 1990, Callaghan, 1991).

Imagine that a spectrum is required from just one of the spheres. If a magnetic field gradient is applied across the sample, then the resonances from the molecules in one sphere will occupy a different band of frequencies from those in the other sphere. If the excitation pulse is made frequency selective, then it will also be spatially selective, and can be used to excite the resonances in one sphere selectively. It has already been seen that the frequency bandwidth of an excitation pulse is inversely proportional to its duration. Therefore, by lengthening the pulse it can be made frequency and, in the presence of a field gradient, spatially selective. Shaping the pulse amplitude can be used to achieve more precise definition of its frequency bandwidth and thus its spatial profile. By combining the pulses with magnetic field gradients applied in three orthogonal directions, a volume can be specified from which signal is acquired. A problem with acquiring spatially localized spectra is that chemical shift and spatial position can become confused. If the resonance of nucleus A, for example, has a significantly different chemical shift or frequency from that of nucleus B, then signal from A will be acquired from a different volume than the signal from B. The problem can be reduced by using larger magnetic field gradients to specify the required volume; nevertheless it remains an important consideration.

The aim of this brief description of the NMR techniques that can be used *in vivo* has been to acquaint the novice with the potential capabilities of these methods to investigate intensive bioreactor systems. What has been achieved so far is discussed in the following.

NMR studies on intensive bioreactor systems

NMR is a tremendously versatile technique for monitoring cellular metabolism and physiology. This versatility stems from its capability to detect a large number of different atomic nuclei that can be found in biological systems. These include ^{1}H, ^{31}P, ^{23}Na, ^{39}K and also non-abundant nuclei, such as ^{13}C and ^{15}N, which can be used for isotope labelling studies of metabolic flux. Furthermore, these measurements may be made non-invasively in anything from isolated cells (Szwergold, 1992; Brindle *et al.*, 1995) perfused organs and animals (Gadian and Radda, 1981; Koretsky and Williams, 1992) to the human being (Radda, 1986; Radda, 1992). The application of NMR to biological systems has been thoroughly reviewed elsewhere and further extensive discussion here would be inappropriate. However, consideration of the still relatively few NMR studies of mammalian cell bioreactors will nevertheless give the reader a good impression of the type of information that can be obtained in this and other biological systems.

CELLULAR ENERGETICS

^{31}P NMR can be used to measure the cellular concentrations of ATP and P_i (see *Figure 2a*) and the intra- and extracellular pHs from the chemical shift of the P_i resonances, if these are resolved. The concentration of free ADP is usually too low in concentration to be detected directly. However, in cells which contain creatine kinase the free cytosolic ADP concentration can be calculated from the observed concentrations of phosphocreatine and ATP and the pH (Brindle *et al.*, 1989; Brindle *et al.*, 1995). The technique thus provides a window on cellular energy status. Studies on skeletal muscle have shown that increased energy demand and thus ATP hydrolysis results in cellular acidosis, decreased phosphocreatine levels and increased ADP concentrations. Similar changes are observed in this tissue and also heart and brain if there is a deficit in ATP production, as would result, for example, from tissue ischaemia.

^{31}P NMR was used to monitor the stability of hybridoma cells in a simple membrane bioreactor (Fernandez *et al.*, 1988). Decreasing dissolved oxygen concentration, by changing the equilibrating gas mixture from 93% O_2 and 7% CO_2 to 8% O_2, 85% N_2 and 7% CO_2, was shown to have no effect on phosphorylated metabolite levels. However, a 30 min period of no perfusion led to splitting of the inorganic phosphate resonance, indicating two pH compartments of substantially different pH. The lower pH compartment was attributed to the extracellular space in the reactor, whereas the higher pH compartment, which did not change in pH during the experiment, was thought to be intracellular. Experiments with an immobilized cell system, showed that superfusion of cells with medium containing either glucose or glutamine as sole carbon source had no effect on the levels of ATP and ADP but that the level of P_i was significantly increased in cells superfused with glutamine alone (Sri-Pathmanathan *et al.*, 1989). It was suggested that the increased P_i might stimulate glutamine utilization

through activation of glutaminase. Hybridoma growth and productivity in a hollow-fibre bioreactor was correlated with cellular energy status, as determined by ^{31}P NMR (Gillies *et al.*, 1991). These measurements were also correlated with the medium feed rate, oxygen tension and lactate/glucose ratio measured in the perfusate. ATP levels were shown to be very dependent upon adequate oxygenation and maintenance of medium pH and declined when the pH was lowered or when there were elevated lactate concentrations. However, it was not known whether these observed changes were due to fluctuations in the intracellular ATP concentration or changes in cell density. High levels of lactate were shown to decrease the transmembrane pH gradient, as determined from splitting of the P_i resonance. Monoclonal antibody productivity correlated with adequate oxygenation, as indicated by increased ATP levels and decreased lactate/glucose ratios.

NMR techniques are being used in the development of an artificial pancreas. ^{31}P NMR was used to monitor the bioenergetics of recombinant insulin-secreting mouse pituitary cells entrapped as spheroids in alginate beads (Constantinidis and Sambanis, 1995). A one-dimensional chemical shift imaging experiment was used to acquire ^{31}P NMR spectra from 0.75 cm thick slices that were orthogonal and parallel to the reactor axis. No significant differences were observed indicating that the cells throughout the reactor were metabolically homogeneous. The technique, however, is not sensitive enough to pick up microscopic metabolic heterogeneity, which is expected to be present within the beads and spheroids due to diffusional limitations. Following 40 days of perfusion there was a sharp increase in medium glucose concentration and a concomitant deterioration in the levels of high energy phosphates as cell death occurred.

A powerful feature of the NMR experiment is its capability, using magnetization transfer techniques, to measure very rapid reactions with rate constants of the order of 0.1–1 s^{-1}. This has been used in ^{31}P NMR studies *in vivo* to measure flux between P_i and ATP and between ATP and phosphocreatine (Brindle, 1988b; Brindle, 1995). Although the fluxes that can be measured are relatively few, the one between P_i and ATP, which in principle gives the ATP turnover rate, is probably the most important one that can be measured in terms of cellular bioenergetics. The technique was used to measure phosphocreatine $\rightarrow$ ATP, $P_i \rightarrow$ ATP and ATP $\rightarrow$ ADP fluxes in immobilized human breast cancer cells (Neeman *et al.*, 1987). Although all kinases will catalyse interconversion of ADP and ATP it was thought likely that adenylate kinase was responsible for most of the observed flux. The apparent ATP synthesis rate (0.2 mM/s) was 50× higher than the oxygen consumption rate (4×10^{-3} mM/s) indicating that aerobic glycolysis was the main pathway of ATP synthesis. While lactate production measurements indicated that this was probably true, this could not necessarily have been deduced from the magnetization transfer measurements. In most tissues the observed flux between P_i and ATP is often not due to unidirectional ATP synthesis and subsequent hydrolysis, but rather is due predominantly to a passive exchange reaction catalysed by the glycolytic enzymes glyceraldehyde 3-phosphate dehydrogenase and phosphoglycerate kinase (Brindle, 1988a). Therefore, except under certain circumstances (Sheldon *et al.*, 1996), this measurement cannot be used to give direct and non-invasive assessment of ATP turnover rate.

The applications of ^{31}P NMR to optimizing bioreactor performance, either as a production system or as an artificial organ, can be summarized as follows. The

technique can be used to measure cell growth, through an increase in ATP signal intensity, and cell death. The latter results in a decrease in cellular energy status (increased Pi concentrations) and subsequently loss of high energy phosphate compounds. The technique can also be used to monitor the adequacy of nutrient provision, both in the reactor as a whole and in specific regions.

PHOSPHOLIPID METABOLISM

^{31}P NMR studies of tumours have often shown growth associated increases in intensity of the phosphomonoester and phosphodiester regions of the spectrum (Radda *et al.*, 1991; Negendank, 1992). The observed phosphomonoesters include phosphocholine and phosphoethanolamine and the diesters include glycerophosphocholine and glycerophosphoethanolamine. Increases in phosphomonoester levels are generally considered to be an indicator of tumour progression and decreases as a sign of a positive response to therapy (Ruiz-Cabello and Cohen, 1992). These changes in phospholipid metabolism are not, however, a unique characteristic of tumour cells as they can also be observed in other rapidly growing tissues such as the regenerating liver and mitogen-stimulated lymphocytes (Dingley *et al.*, 1992; Murphy *et al.*, 1992). There have been numerous studies of phospholipid metabolism in cultured mammalian cells in which the aim has been to elucidate the biochemistry underlying these changes (Daly and Cohen, 1989; Ruiz-Cabello and Cohen, 1992). In the context of intensive mammalian cell bioreactor systems, studies of phospholipid metabolism may be useful in assessing the proliferative capacity of the culture. However it must be emphasized that the correlation that has been observed between proliferation and the levels of phosphomonester and diester compounds is not absolute (Ruiz-Cabello and Cohen, 1992). Some of the studies which have been carried out in intensive reactor systems are discussed in the following.

Phosphocholine levels were shown to decline and phosphoethanolamine levels increase during growth of two rat glioma cell lines in hollow fibre bioreactors (Gillies *et al.*, 1994). The phosphocholine levels were lower and phosphoethanolamine levels higher in stationary phase cells as compared to log phase cells. Although this change was not observed in a study of recombinant mouse pituitary cells (see above), where the PC/PE ratio remained constant throughout the culture (Constantinidis and Sambanis, 1995), it has been observed in other cells (Ronen *et al.*, 1990; Freyer *et al.*, 1991). The increased phosphocholine levels in proliferating cells may be the result of increased choline uptake and phosphorylation, or alternatively a consequence of elevated phospholipase C activity (Daly *et al.*, 1987; Murphy *et al.*, 1992). The origin of phosphoethanolamine in the glioma cells was not established but may be the result of phospholipase activation. It has been shown that activation of phospholipases, in cells treated with fatty acids, can result in the accumulation of phosphoethanolamine (Gillham and Brindle, 1996). Since these fatty acids also induce the formation of cytoplasmic lipid droplets, which are known to accumulate in rapidly growing cells, this suggests that the appearance of phosphoethanolamine in stationary phase cells could be the result of fatty acid uptake and consequent stimulation of phospholipases.

The effects of acidosis on phospholipid metabolism were studied in three different mammalian cell lines growing in hollow fibre bioreactors (Galons *et al.*, 1995). In all three there was a decline in the level of phosphocholine and an increase in the

concentration of glycerophosphocholine. It was thought likely that this was the result of increased phosphatidylcholine breakdown via activation of phospholipase A_2 and lysophospholipase and inhibition of glycerophosphocholine phosphodiesterase activity.

CARBON METABOLISM

Administration of a ^{13}C label and subsequent detection of its redistribution amongst cellular metabolites, using ^{13}C NMR, has been used since the earliest days of *in vivo* NMR to monitor carbon fluxes in metabolic pathways (Shulman *et al.*, 1979). Initially, these experiments were carried out with micro-organisms but today they are also being used on human beings, most notably to study glycogen metabolism (Shulman *et al.*, 1995). ^{13}C NMR detection of a ^{13}C label has a number of advantages over more traditional studies with the radioactive label, ^{14}C. The ^{13}C NMR spectrum not only shows which metabolite is labelled but also which carbon in the metabolite is labelled. Contrast this with radiotracer studies where first the tissue must be extracted and the labelled metabolites chromatographically separated before counting. If the position of the label in a molecule is to be determined, then the separated metabolite will need to be further degraded and the fragments separated. When the NMR measurements are made non-invasively they also allow serial measurements of labelling in an intact tissue. Another advantage of NMR detection of a ^{13}C label is that the technique can detect whether adjacent carbons in a molecule are labelled, due to mutual splitting of their resonance lines. This can be of enormous value in determining relative fluxes in different pathways (Jeffrey *et al.*, 1991, Szyperski *et al.*, 1996). Note that the probability of adjacent carbons becoming labelled with ^{13}C is quite high as the fractional labelling of the added substrates is also relatively high. With radioactively labelled substrates the fractional labelling is usually very low as the sensitivity of detection is much higher. The sensitivity of detection of the ^{13}C label can be enhanced to some extent if it is detected indirectly in the ^{1}H NMR spectrum. This has the added advantage that the fractional labelling of the molecule may also be determined (see above). The study of carbon metabolism in intensive mammalian cell bioreactors using ^{13}C NMR is discussed in the following.

^{13}C NMR was used to monitor the metabolism of [1-^{13}C]glucose by hybridoma cells in a simple membrane bioreactor (Fernandez *et al.*, 1988). In addition to the signal from glucose, signals from the methyl carbons of lactate and alanine were also observed. A step change in the concentration of glucose from 2 mM to 10 mM resulted in a sharp increase in the concentration of labelled lactate. The concentrations of intra- and extracellular lactate were determined by comparing spectra from the reactor with those of the media. The intracellular concentrations of lactate and alanine were shown to be significantly higher than the extracellular concentrations. A similar but more comprehensive set of experiments was carried out on hybridoma cells growing in a hollow fibre bioreactor (Mancuso *et al.*, 1994). The cells were serially infused with [1-^{13}C]glucose, [2-^{13}C]glucose and [3-^{13}C]glutamine. Measurements on the reactor, in conjunction with off-line measurements on the medium, were used to determine the intracellular concentrations of several metabolites and also the fluxes in several metabolic pathways. The major conclusions were that flux in the pentose phosphate pathway was very small compared to that in glycolysis, a significant amount of

glutamine was converted to pyruvate via malate and that most of the pyruvate carbon that enters the TCA cycle does so via pyruvate dehydrogenase. There was no detectable flux of pyruvate carbon through pyruvate carboxylase. In these experiments the intracellular volume in the reactor was determined from ^{31}P NMR measurements of the ATP concentration in the reactor and from ^{23}Na NMR measurements of the intra- and extracellular sodium concentrations (see below).

NITROGEN METABOLISM

Nitrogen metabolism can be monitored in cultured cells using ^{15}N NMR. This has an advantage over radiotracer studies in that there is no readily available radioactive isotope, although there have been a few studies using the short-half life, positron-emitting isotope, ^{13}N ($t_{1/2} = 9.96$ min). ^{15}N NMR however is even less sensitive than ^{13}C NMR (see *Table 1*). Again a significant improvement in sensitivity can be effected by detecting the ^{15}N label indirectly via spin-coupled protons (Street *et al.*, 1993). L[2-^{15}N]glutamine was added to cultures of hybridoma cells and ^{15}N-labelled alanine detected using ^{15}N NMR measurements on concentrated supernatants (Fernandez *et al.*, 1988). ^{1}H/^{15}N NMR indirect detection experiments were used to monitor the metabolic fate of glutamine and ammonia nitrogen in four different mammalian cell lines (Street *et al.*, 1993). Glutamine amine nitrogen was found predominantly in alanine and also in aspartate and glycine. There was no detectable formation of ammonia from this nitrogen, showing that most of the glutamate formed in the reaction catalysed by glutaminase was subsequently transaminated, rather than oxidatively deaminated by glutamate dehydrogenase. The amide nitrogen of glutamine on the other hand was converted predominantly to ammonia. Glutamine synthesis from ammonia was only observed in cells expressing relatively high levels of glutamine synthetase. This study was again performed on cell supernatants. However the improved sensitivity offered by indirect detection make it possible, at least in principle, to perform these experiments on a bioreactor.

FLOW

NMR imaging experiments are frequently flow sensitive in that magnetization is created and then detected some time later, typically a few tens of milliseconds. If a spin moves during this time then its signal intensity in the resulting image may be altered (see *Figure 4a*). The flow sensitivity of the experiment can be enhanced by the application of appropriate magnetic field gradients during this time delay between signal creation and detection. NMR flow imaging techniques were used to measure flow in a cell-free hollow fibre bioreactor (Hammer *et al.*, 1990). As well as measuring flow within the fibres convective or Starling flow was also measured in the extracapillary space. It was anticipated that this type of experiment would facilitate optimisation of bioreactor operating conditions and improve the design of these devices. Similar flow imaging experiments were used to determine the location of cell masses in a cell-filled hollow fibre bioreactor (Donoghue *et al.*, 1992). Those regions in which there was low flow were thought to contain cell mass. An obvious disadvantage of this approach is that there may be regions in which flow is restricted for other reasons but which would appear as if cell mass were present.

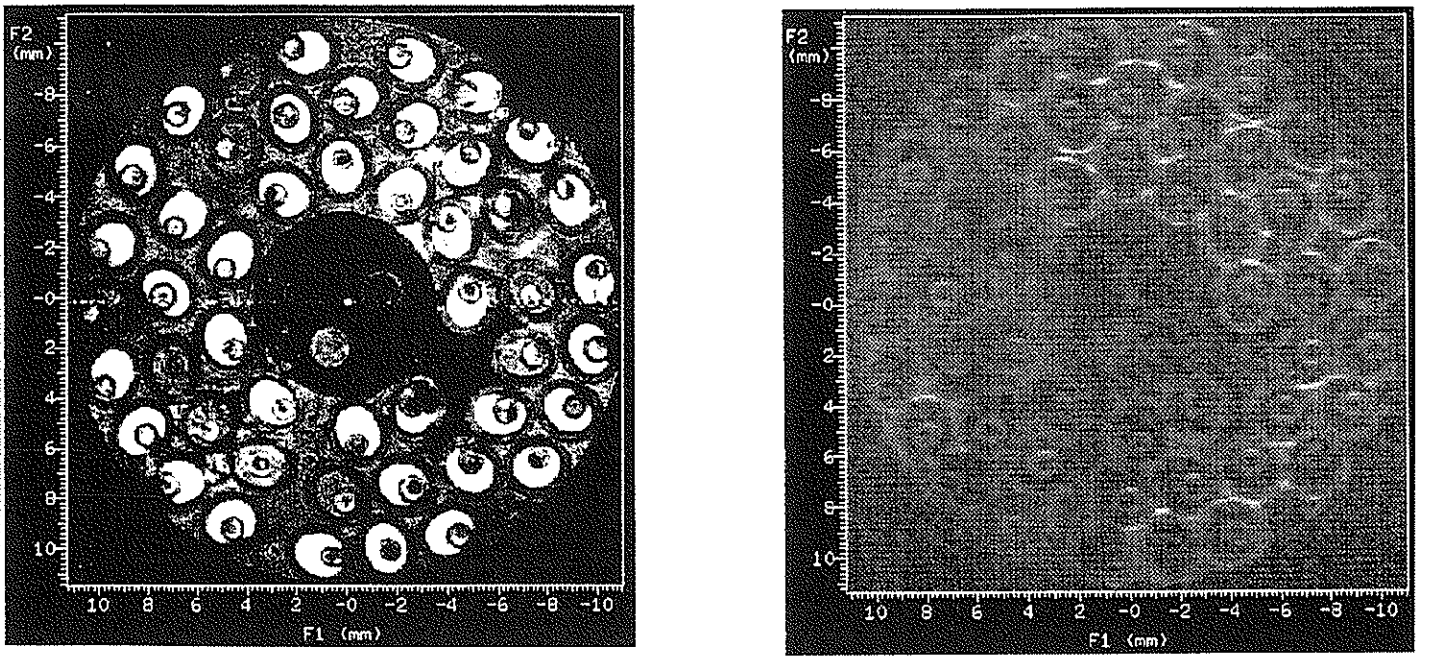

Figure 4. (a) ^{1}H image acquired from a transverse section of a hollow-fibre bioreactor. The signal in the image is from water protons. Medium was perfused through the fibre-within-fibre pairs, while the cells grew in the extracapillary space. The high signal intensity within some of the larger fibres was due to the effects of medium flow. Experiments similar to this have been used to measure medium flow rates in a hollow-fibre bioreactor (Hammer *et al.*, 1990). (b) Diffusion-weighted ^{1}H image acquired from the same transverse section of the reactor that was show in (a). Intracellular water molecules and water molecules within the fibre walls have a lower apparent diffusion coefficient (ADC) than water molecules elsewhere. In a diffusion-weighted image these water molecules, with low ADC values, give higher signal intensities. The highest signal intensities, observed around the outside of some of the larger fibres, has been assigned to cell masses (Callies *et al.*, 1994, Williams *et al.*, 1997).

CELL VOLUME

Quantitative metabolic measurements on an intensive bioreactor require an estimate of the cell volume. A commonly used non-invasive approach has been to estimate the volume from nutrient uptake rates. However, this assumes constant specific consumption rates during the reactor run, an assumption which may not always be justified (Mancuso *et al.*, 1990).

The intracellular volume of hybridomas growing in a hollow fibre bioreactor was estimated by using ^{23}Na NMR to measure the total sodium ion concentration in the reactor (Mancuso *et al.*, 1990). As the intracellular sodium ion concentration (~ 7 mM) was much less than the extracellular concentration (158 mM), the increase in cell volume, resulting from cell growth, could be determined from the decrease in the sodium NMR signal from the reactor. The cell volume estimated in this way showed good agreement with that determined from oxygen consumption measurements and from ^{31}P NMR measurements of nucleoside triphosphate content. The hybridoma cell volume in a hollow fibre bioreactor has also been estimated by measuring the ratio of intra- and extracellular sodium ion concentrations (Gillies *et al.*, 1991). The NMR resonance of extracellular sodium was separated from the intracellular resonance by adding a 'shift reagent' to the extracellular space. This agent, as its name implies, shifts the frequency of those sodium nuclei with which it comes into contact, in this case the extracellular sodium ions. By measuring the intracellular sodium ion concentration, in a separate experiment outside the reactor, they were able to estimate the total intracellular volume in the reactor, from the NMR measurements of the ratio of intra- and extracellular sodium ion concentrations.

The intracellular volume of mammalian cells growing in HFBRs has also been estimated by using dimethyl methylphosphonate (DMMP) as a ^{31}P NMR probe of cell volume (Barry *et al.*, 1993). This small, non-toxic and uncharged molecule, which diffuses passively across the plasma membrane, shows separate ^{31}P resonances for the intra- and extracellular molecules. The lower frequency chemical shift inside the cells is due to a reduction in hydrogen bonding between water and the DMMP. By measuring the T_1 values for the intra- and extracellular resonances, the partially saturated DMMP peaks in ^{31}P NMR spectra of HFBRs could be corrected to give the relative volumes of the intra- and extracellular compartments.

The lower apparent diffusion coefficient (ADC) of intracellular water molecules was exploited to estimate the intracellular water fraction in immobilized breast cancer cells (van Zijl *et al.*, 1991). In a diffusion-weighted spectroscopy experiment the signal intensity is a function of the diffusion time and the size and duration of the diffusion gradients. A plot of the natural logarithm of signal intensity versus size of the diffusion gradient gave a bi-exponential plot, indicating two components of differing ADC. The slopes of these components could be used to estimate the ADC values of the intracellular and extracellular water molecules and the intercepts of their asymptotes could be used to estimate the intra- and extracellular water fractions. However this estimate assumes that the relaxation times of intra- and extracellular water molecules are either known or the experiments are performed under conditions such that any differences in relaxation times can be ignored.

This diffusion-weighted spectroscopy experiment was incorporated into an imaging pulse sequence in order to distinguish a rim of viable cells in multicellular tumour

spheroids from a necrotic core region (Neeman *et al.*, 1991). The water in the cells had a much lower ADC than the surrounding interstitial water and the water in the necrotic core. A similar experiment has been used to map the growth and distribution of CHO cells in a HFBR (Callies *et al.*, 1994). A conventional, non-diffusion-weighted image, showed the distribution of the hollow fibres in the reactor but could not show where the cells were located. However the cells were clearly visible in a diffusion-weighted image (see *Figure 4b*). The assignment of the water fraction with low ADC in these images to intracellular water was confirmed by acquiring spatially localized ^{1}H spectra. Regions of the reactor in which the water had a low ADC also gave ^{1}H spectra which contained cellular lipid signals. This experiment appears to have some potential for monitoring the effect of bioreactor design and operation strategies on the subsequent colonisation and growth of cells in specific regions of the reactor. It should also be capable of providing quantitative measurements of total cell volume in these regions.

OXYGEN TENSION

The spin lattice relaxation times or T_1s of the fluorine nuclei in some perfluorocarbons have been shown to be linearly dependent on the dissolved oxygen concentration (Shukla *et al.*, 1995). This property has been exploited to produce ^{19}F NMR probes of dissolved oxygen concentrations *in vivo*. Intravenous injection of a perfluorocarbon emulsion and subsequent non-invasive ^{19}F NMR measurements have been used to measure oxygen tension in a variety of tissues (Dardzinski and Sotak, 1994, Noth *et al.*, 1995). The oxygen concentration available to cells immobilized in a gel matrix was determined by measuring the T_1s of fluorine nuclei in a perfluorocarbon that had been incorporated into the gel matrix (McGovern *et al.*, 1993). In the presence of cells there was a substantial reduction in the dissolved oxygen concentration in the reactor. The extracapillary space in a hollow fibre bioreactor has been loaded with a perfluorocarbon emulsion and a ^{19}F NMRT_1 imaging experiment used to measure the regional distribution of dissolved oxygen in the reactor (Williams *et al.*, 1997). Cell distribution was also measured using diffusion-weighted imaging (see above) and it showed that there was a correlation between dissolved oxygen concentration and cell density. The cells tended to grow around the fibres and in regions in which the cell density was high the dissolved oxygen concentration was reduced. Experiments of this type should assist in the development of bioreactor design and operation strategies which minimize the formation of oxygen gradients.

Conclusions

A primary aim of this brief review has been to alert the novice to the potential of NMR techniques for monitoring the performance of intensive mammalian cell bioreactors. Applications to the hollow-fibre have been concentrated on as this seems to have been the most widely studied system so far. The imaging techniques for measuring medium flow, cell distribution and oxygen tension, when coupled with localized spectroscopy techniques for measuring regional cell metabolism, would seem to constitute a very powerful methodological approach. In the context of artificial organs, the application of NMR techniques appears to be particularly attractive. The application of multi-

nuclear NMR techniques to the study of intact biological systems, including man, over the last 20 years means that there is wealth of data on what the NMR spectra of a variety of tissues look like in health and disease. This database could be very useful in assessing the performance of cells from these tissues when they are incorporated into a bioartificial organ. For example, there have been several ^{13}C NMR studies of gluconeogenesis and glycogen synthesis in the liver *in vivo* (Cohen, 1987; Shulman *et al.*, 1988). These same experiments could be used to assess liver function in an hepatocyte-based artificial liver. The potential, however, of NMR to examine bioartificial organ performance goes beyond simple measurements on the isolated device. Yarmush and co-workers (Foy *et al.*, 1994) used ^{31}P NMR to assess the energy status of hepatocytes during their isolation from the animal. In this way they were able to optimise the liver perfusion protocol used in the isolation procedure. This approach could be taken a step further, in the case of implanted devices, by using NMR to non-invasively monitor the performance of the resultant device when this is subsequently implanted in the patient. There is a precedent for this in that ^{31}P NMR has been used to monitor the subsequent performance of implanted organs (Haug *et al.*, 1988). This approach could be useful, for example, to monitor the progress of skin grafts. ^{31}P NMR could be used to monitor the metabolism of skin cells in culture (Langer and Vacanti, 1993) and following their subsequent grafting onto the patient (Bohning *et al.*, 1996). Although this is speculative, it nevertheless illustrates the potential of the method.

Acknowledgements

I would like to thank the BBSRC and the EC for supporting work in this area in my laboratory. I would also like to thank Sandra Fulton for her suggestions for improving the manuscript and Shane Williams and Maria Anthony for *Figure* 2 and *Figure* 4.

References

ARATHOON, W.R. AND BIRCH, J.R. (1986). Large-scale cell culture in biotechnology. *Science (Washington, DC)* **232**, 1390–1395.

BALABAN, R.S. (1984). The application of nuclear magnetic resonance to the study of cellular physiology. *American Journal of Physiology* **246**, C10–C19.

BARRY, J.A., MCGOVERN, K A., LIEN, Y-H.H., ASHMORE, B. AND GILLIES, R.J. (1993). Dimethyl methylphosphonate (DMMP): A ^{31}P nuclear magnetic resonance spectroscopic probe of intracellular volume in mammalian cell cultures. *Biochemistry* **32**, 4665–4670.

BOHNING, D.E., WRIGHT, A.C. AND SPICER, K.M. (1996). *In vivo* phosphorus spectroscopy of human skin. *Magnetic Resonance in Medicine* **35**, 186–193.

BORYS, M.C., LINZER, D.I H. AND PAPOUTSAKIS, E.T. (1993). Culture pH affects expression rates and glycosylation of recombinant mouse placental lactogen proteins by Chinese Hamster ovary (CHO) cells. *Bio/Technology* **11**, 720–724.

BRINDLE, K.M. (1988a). ^{31}P NMR magnetization-transfer measurements of flux between inorganic phosphate and adenosine 5'-triphosphate in yeast cells genetically modified to overproduce phosphoglycerate kinase. *Biochemistry* **27**, 6187–6196.

BRINDLE, K.M. (1988b). NMR methods for measuring enzyme kinetics *in vivo*. *Progress in Nuclear Magnetic Resonance Spectroscopy* **20**, 257–293.

BRINDLE, K.M. (1995). Enzyme-catalyzed exchange: magnetization transfer measurements. *In Encyclopedia of Nuclear Magnetic Resonance*, ed. D.M. Grant and R.K. Harris, pp. 1902–1909. Chichester, UK: John Wiley and Sons Ltd.

BRINDLE, K.M., BLACKLEDGE, M.J., CHALLISS, R.A.J. AND RADDA, G.K. (1989). ^{31}P NMR

magnetization-transfer measurements of ATP turnover during steady-state isometric muscle contraction in the rat hind limb *in vivo*. *Biochemistry* **28**, 4887–4893.

BRINDLE, K.M., BOYD, J., CAMPBELL, I.D., PORTEOUS, R. AND SOFFE, N. (1982). Observation of carbon labelling in cell metabolites using proton spin echo NMR. *Biochemical and Biophysical Research Communications* **109**, 864–871.

BRINDLE, K.M., FULTON, A.M. AND WILLIAMS, S-P. (1995). Studies of cellular energetics using ^{31}P NMR. In *Bioenergetics. A Practical Approach*, ed. G.C. Brown and C. E. Cooper, pp. 159–182. Oxford, New York, Tokyo; Oxford University Press.

CALLAGHAN, P.T. (1991). *Principles of Nuclear Magnetic Resonance Microscopy*. Oxford: Oxford University Press.

CALLIES, R., JACKSON, M.E. AND. BRINDLE, K.M (1994). Measurements of the growth and distribution of mammalian cells in a hollow-fiber bioreactor using nuclear magnetic resonance imaging. *Bio/Technology* **12**, 75–78.

CHRESAND, T.J., GILLIES, R.J. AND DALE, B.E. (1988). Optimum fiber spacing in a hollow fiber bioreactor. *Biotechnology and Bioengineering* **32**, 983–992.

COHEN, S. (1987). ^{13}C and ^{31}P NMR study of gluconeogenesis: Utilization of ^{13}C labeled substrates by perfused liver from streptozotocin-diabetic and untreated rats: ^{13}C NMR assay of pyruvate kinase flux. *Biochemistry* **26**, 573–580.

CONSTANTINIDIS, I. AND SAMBANIS, A. (1995). Towards the development of artificial endocrine tissues: ^{31}P NMR spectroscopic studies of immunoisolated, insulin-secreting AtT-20 cells. *Biotechnology and Bioengineering* **47**, 431–443.

DALY, P.F. AND COHEN, J.S. (1989). Magnetic resonance spectroscopy of tumours and potential *in vivo* clinical applications: a review. *Cancer Research* **49**, 770–779.

DALY, P.F., LYON, R.C., FAUSTINO, P.J. AND COHEN, J.S. (1987). Phospholipid metabolism in cancer cells monitored by ^{31}P NMR spectroscopy. *Journal of Biological Chemistry* **262**, 14875–14878.

DARDZINSKI, B.J. AND SOTAK, C.H. (1994). Rapid tissue oxygen tension mapping using ^{19}F inversion-recovery echo-planar imaging of perfluoro-15-crown-ether. *Magnetic Resonance in Medicine* **32**, 88–97.

DEROME, A.E. (1987). *Modern NMR Techniques for Chemistry Research*. Oxford: Pergamon Books Ltd.

DINGLEY, A.J., KING, N.J.C. AND KING, G.F. (1992). An NMR investigation of the changes in plasma membrane triglyceride and phospholipid precursors during activation of T-lymphocytes. *Biochemistry* **31**, 9098–9106.

DONOGHUE, C., BRIDEAU, M., NEWCOMER, P., PANGRLE, B., DIBIASIO, D., WALSH, E. AND MOORE, S. (1992). Use of magnetic resonance imaging to analyze the performance of hollow-fiber bioreactors. *Annals of the NY Academy of Sciences* **665**, 285–300.

DRURY, D.D., DALE, B.E. AND GILLIES, R.J. (1988). Oxygen transfer properties of a bioreactor for use within a nuclear magnetic resonance spectrometer. *Biotechnology and Bioengineering* **32**, 966–974.

FERNANDEZ, E.J. (1996). Nuclear magnetic resonance spectroscopy and imaging. In *Immobilised Living Cell Systems: Modelling and Experimental Methods*, ed. R.G. Willaert, G.V. Baron and L. De Backer. Chichester, UK: John Wiley.

FERNANDEZ, E.J., MANCUSO, A. AND CLARK, D.S. (1988). NMR spectroscopy studies of hybridoma metabolism in a simple membrane reactor. *Biotechnology Progress* **4**, 173–183.

FOY, B.D., TONER, M., TOMPKINS, R.G. AND YARMUSH, M.L. (1994). Engineering organ perfusion protocols: NMR analysis of hepatocyte isolation from perfused rat liver. *Biotechnology and Bioengineering* **43**, 661–672.

FREYER, J P., SCHOR, P.L., JARRETT, K.A., NEEMAN, M. AND SILLERUD, L.O. (1991). Cellular energetics measured by phosphorus nuclear magnetic resonance spectroscopy are not correlated with chronic nutrient deficiency in multicellular tumor spheroids. *Cancer Research* **51**, 3831–3837.

GADIAN, D.G. (1995). *NMR and its Applications to Living Systems*. Oxford: Oxford University Press.

GADIAN, D.G. AND RADDA, G.K. (1981). NMR studies of tissue metabolism. *Annual Reviews in Biochemistry* **50**, 69–83.

GALONS, J-P., JOB, C. AND GILLIES, R.J. (1995). Increase of GPC levels in cultured mammalian cells during acidosis. A ^{31}P MR spectroscopy study using a continous bioreactor system. *Magnetic Resonance in Medicine* **33**, 422–426.

GILLHAM, H. AND BRINDLE, K.M. (1996). ^{31}P NMR measurements of the effects of unsaturated fatty acids on cellular phospholipid metabolism. *Magnetic Resonance in Medicine* **35**, 481–488.

GILLIES, R.J., BARRY, J.A. AND ROSS, B.D. (1994). *In vitro* and *in vivo* ^{13}C and ^{31}P NMR analyses of phosphocholine metabolism in rat glioma cells. *Magnetic Resonance in Medicine* 32, 310–318.

GILLIES, R.J., MACKENZIE, N.E. AND DALE, B.E. (1989). Analyses of bioreactor performance by nuclear magnetic resonance spectroscopy. *Bio/Technology* **7**, 50–54.

GILLIES, R.J., SCHERER, P.G., RAGHUNAND, N., OKERLUND, L.S., MARTINEZ-ZAGUILAN, R., HESTERBERG, L. AND. DALE, B.E (1991). Iteration of hybridoma cell growth and productivity in hollow fiber bioreactors using ^{31}P NMR. *Magnetic Resonance in Medicine* **18**, 181–192.

GLACKEN, M.W., FLEISCHAKER, R.J. AND SINSKEY, A.J. (1983). Large-scale production of mammalian cells and their products: engineering principles and barriers to scale-up. *Annals of the NY Academy of Sciences* **413**, 355–373.

HAMMER, B.E., HEATH, C.A., MIRER, S.D. AND BELFORT, G. (1990). Quantitative flow measurements in bioreactors by nuclear magnetic resonance imaging. *Bio/Technology* **8**, 327–330.

HAUG, C.E., SHAPIRO, J.I., COSBY, R.L., CHAN, L. AND WEIL, R. (1988). P-31 nuclear magnetic-resonance spectroscopy of heart, heart-lung, and kidney allograft-rejection in the rat. *Transplant Proceedings* **20**, 848–855.

HAYTER, P.M., CURLING, E.M.A., GOULD, M.L., BAINES, A.J., JENKINS, N., SALMON, I., STRANGE, P.G. AND BULL, A.T. (1993). The effect of the dilution rate on CHO cell physiology and recombinant interferon production in glucose-limited chemostat culture. *Biotechnology and Bioengineering* **42**, 1077–1085.

HIMMELFARB, P., THAYER, P.S. AND MARTIN, H.E. (1969). Spin-filter culture: the propagation of mammalian cels in suspension. *Science (Washington, DC)* **164**, 555–557.

HUBBELL, J.A. AND LANGER, R. (1995). Tissue engineering. *Chemical Engineering News* **73**, 42–54.

JAMES, T.L. (1975). *Nuclear Magnetic Resonance in Biochemistry: Principles and Applications*. New York: Academic Press.

JAUREGUI, H.O., CHOWDHURY, N.R. AND CHOWDHURY, J.R. (1996). Use of mammalian liver cells for artificial liver support. *Cell Transplantation.* **5**, 353–367.

JEFFREY, F.M.H., RAJAGOPAL, A., MALLOY, C.R. AND SHERRY, A.D. (1991). ^{13}C NMR: A simple yet comprehensive method for analysis of intermediary metabolism. *Trends in Biochemical Science* **16**, 5–10.

KAMLOT, A., ROZGA, J., WATANABE, F.D. AND DEMETRIOU, A.A. (1996). Artificial liver support systems. *Biotechnology and Bioengineering* **50**, 382–391.

KNIGHT, P. (1989). Hollow fiber bioreactors for mammalian cell culture. *Bio/Technology* **7**, 459–461.

KORETSKY, A.P. AND WILLIAMS, D.S. (1992). Application of localized *in vivo* NMR to whole organ physiology in the animal. *Annual Reviews in Physiology* **54**, 799–826.

KUHN, W. (1990). NMR microscopy – Fundamentals, limits and possible applications. *Angewandte Chemie International Edition English* **29**, 1–19.

LANGER, R. AND VACANTI, J.P. (1993). Tissue engineering. *Science (Washington, DC)* **260**, 920–926.

LANGER, R. AND VACANTI, J.P. (1995). Artificial organs. *Scientific American* **273**, 100–103.

MANCUSO, A., FERNANDEZ, E.J., BLANCH, H.W. AND CLARK, D.S. (1990). A nuclear magnetic resonance technique for determining hybridoma cell concentration in hollow fiber bioreactors. *Bio/Technology* **8**, 1282–1285.

MANCUSO, A., SHARFSTEIN, S.T., TUCKER, S.N., CLARK, D.S. AND BLANCH, H.W. (1994). Examination of primary metabolic pathways in a murine hybridoma with carbon-13 nuclear magnetic resonance spectroscopy. *Biotechnology and Bioengineering* **44**, 563–585.

MASSON, S. AND QUISTDORFF, B. (1992). The ^{31}P NMR visibility of ATP in perfused rat liver remains about 90 per cent, unaffected by changes of metabolic state. *Biochemistry* **31**, 7488–7493.

MCGOVERN, K.A., SCHOENIGER, J.S., WEHRLE, J.P., NG, C.E. AND GLICKSON, J.D. (1993). Gel-entrapment of perfluorocarbons: a fluorine-19 NMR spectroscopic method for monitoring oxygen concentration in cell perfusion systems. *Magnetic Resonance in Medicine* **29**, 196–204.

MURPHY, E., GABEL, S.A., FUNK, A. AND LONDON, R.E. (1988). NMR observability of ATP: preferential depletion of cytosolic ATP during ischemia in perfused rat liver. *Biochemistry* **27**, 526–528.

MURPHY, E.J., BRINDLE, K.M., RORISON, C.J., DIXON, R.M., RAJAGOPALAN, B. AND RADDA, G.K. (1992). Changes in phosphatidylethanolamine metabolism in regenerating rat liver as measured by ^{31}P NMR. *Biochimica et Biophysica Acta* **1135**, 27–34.

MURPHY, E.J., RAJAGOPALAN, B., BRINDLE, K.M. AND RADDA, G.K. (1989). Phospholipid bilayer contribution to ^{31}P NMR spectra *in vivo*. *Magnetic Resonance in Medicine* **12**, 282–289.

NEEMAN, M., JARRETT, K.A., SILLERUD, L.O. AND FREYER, J.P. (1991). Self-diffusion of water in multicellular spheroids measured by magnetic resonance microimaging. *Cancer Research* **51**, 4072–4079.

NEEMAN, M., RUSHKIN, E., KAYE, A.M. AND DEGANI, H. (1987). ^{31}P NMR studies of phosphate transfer rates in T47D human breast cancer cells. *Biochimica et Biophysica Acta* **930**, 179–192.

NEGENDANK, W. (1992). Studies of human tumours by MRS: a review. *NMR Biomedicine* **5**, 303–324.

NOTH, U., MORRISSEY, S.P., DEICHMANN, R., ADOLF, H., SCHWARZBAUER, C., LUTZ, J. AND HAASE, A. (1995). *In vivo* measurement of partial oxygen pressure in large vessels and in the reticuloendothelial system using fast 19F-MRI. *Magnetic Resonance in Medicine* **34**, 738–745.

PENG, C-A. AND PALSSON, B.O. (1996). Determination of specific oxygen uptake rates in human hematopoietic cultures and implications for bioreactor design. *Annals in Biomedical Engineering* **24**, 373–381.

PIRET, J.M. AND COONEY, C.L. (1990a). Mammalian cell and protein distributions in ultrafiltration hollow fiber bioreactors. *Biotechnology and Bioengineering* **36**, 902–910.

PIRET, J.M. AND COONEY, C.L. (1990b). Model of oxygen transport limitations in hollow fiber bioreactors. *Biotechnology and Bioengineering* **37**, 80–92.

PYKETT, I.L. (1982). NMR imaging in medicine. *Scientific American* **246**, 78.

RADDA, G.K. (1986). The use of NMR spectroscopy for the understanding of disease. *Science (Washington, DC)* **233**, 640–645.

RADDA, G.K. (1992). Control, bioenergetics, and adaptation in health and disease – noninvasive biochemistry from nuclear magnetic resonance. *FASEB Journal* **6**, 3032–3038.

RADDA, G.K., DIXON, R.M. AND WOOD, C.A. (1991). N.M.R. studies of phospholipid metabolism and cell proliferation. *Biochemical Society Transactions* **19**, 995–996.

RONEN, S.M., STIER, A. AND DEGANI, H. (1990). NMR studies of the lipid metabolism of T47D human breast cancer spheroids. *FEBS Letters* **266**, 147–149.

ROTEM, A., TONER, M., BHATIA, S., FOY, B.D., TOMPKINS, R.G. AND YARMUSH, M.L. (1994). Oxygen is a factor determining *in vitro* tissue assembly: Effects on attachment and spreading of hepatocytes. *Biotechnology and Bioengineering* **43**, 654–660.

ROTEM, A., TONER, M., TOMPKINS, R.G. AND YARMUSH, M.L. (1992). Oxygen uptake in cultured hepatocytes. *Biotechnology and Bioengineering* **40**, 1286–1291.

ROTHMAN, D.L., NOVOTNY, E.J., SHULMAN, G.I., HOUSEMAN, A.M., PETROFF, O.A C., MASON, G., NIXON, T., HANSTOCK, C.C., PRICHARD, J.W. AND SHULMAN, R.G. (1992). ^{1}H-[^{13}C]NMR measurements of [4-^{13}C]glutamate turnover in human brain. *Proceedings of the National Academy of Sciences, USA* **89**, 9603–9606.

RUIZ-CABELLO, J. AND COHEN, J.S. (1992). Phospholipid metabolites as indicators of cancer cell function. *NMR in Biomedicine* **5**, 226–233.

SANDERS, J.K.M. AND HUNTER, B.K. (1987). Modern NMR Spectroscopy. Oxford: Oxford University Press.

SARDONINI, C. AND DIBIASIO, D. (1992). An investigation of the diffusion-limited growth of animal cells around single hollow fibers. *Biotechnology and Bioengineering* **40**, 1233–1242.

SHELDON, J.G., WILLIAMS, S-P., FULTON, A.M. AND BRINDLE, K.M. (1996). 31P NMR magnetization transfer study of the control of ATP turnover in *Saccharomyces cerevisiae*. *Proceedings of the National Academy of Sciences, USA* **93**, 6399–6404.

SHI, Y., RYU, D.D.Y. AND PARK, S.H. (1993). Monoclonal antibody productivity and metabolic pattern of perfusion cultures under varying oxygen tensions. *Biotechnology and Bioengineering* **42**, 430–439.

SHUKLA, H., MASON, R.P., WOESSNER, D.E. AND ANTICH, P.P. (1995). A comparison of three commercial perfluorocarbon emulsions as high-field ^{19}F NMR probes of oxygen tension and temperature. *Journal of Magnetic Resonance* **106**, 131–141.

SHULMAN, G.I., ROTHMAN, D.L., CHUNG, Y., ROSSETTI, L., PETIT, W., BARRETT, E.J. AND SHULMAN, R.G. (1988). ^{13}C NMR studies of glycogen turnover in the perfused rat liver. *Journal of Biological Chemistry* **263**, 5027–5029.

SHULMAN, R.G., BLOCH, G. AND ROTHMAN, D.L. (1995). *In vivo* regulation of muscle glycogen synthase and the control of glycogen synthesis. *Proceedings of the National Academy of Sciences, USA* **92**, 8535–8542.

SHULMAN, R.G., BROWN, T.R., UGURBIL, K., OGAWA, S., COHEN, S.M. AND DEN HOLLANDER, J.A. (1979). Cellular applications of ^{31}P and ^{13}C nuclear magnetic resonance. *Science (Washington, DC)* **205**, 160–166.

SRI-PATHMANATHAN, R.M., BRADDOCK, P. AND BRINDLE, K.M. (1989). ^{31}P NMR studies of glucose and glutamine metabolism in cultured mammalian cells. *Biochimica et Biophysica Acta* **1051**, 131–137.

STREET, J.C., DELORT, A-M., BRADDOCK, P.S.H. AND BRINDLE, K.M. (1993). A $^{1}H/^{15}N$ n.m.r. study of nitrogen metabolism in cultured mammalian cells. *Biochemical Journal* **291**, 485–492.

SZWERGOLD, B.S. (1992). NMR spectroscopy of cells. *Annual Reviews in Physiology* **54**, 775–798.

SZYPERSKI, T., J.E. BAILEY, AND K. WUTHRICH. (1996). Detecting and dissecting metabolic fluxes using biosynthetic fractional labeling and two dimensional NMR spectroscopy. *TIBTECH.* **14**, 453–459.

VAN ZIJL, P.C.M., MOONEN, C.T.W., FAUSTINO, P., PEKAR, J., KAPLAN, O. AND COHEN, J.S. (1991). Complete separation of intracellular and extracellular information in NMR spectra of perfused cells by diffusion-weighted spectroscopy. *Proceedings of the National Academy of Sciences, USA* **88**, 3228–3232.

WILLIAMS, S.N.O., RAINER, R.M. AND BRINDLE, K.M. (1997). Mapping of oxygen tension and cell distribution in a hollow fiber bioreactor using magnetic resonance imaging. *Biotechnology and Bioengineering* **56**, 56–61.

YARMUSH, M.L., DUNN, J.C.Y. AND TOMPKINS, R.G. (1992). Assessment of artificial liver support technology. *Cell Transplantation* **1**, 323–341.